

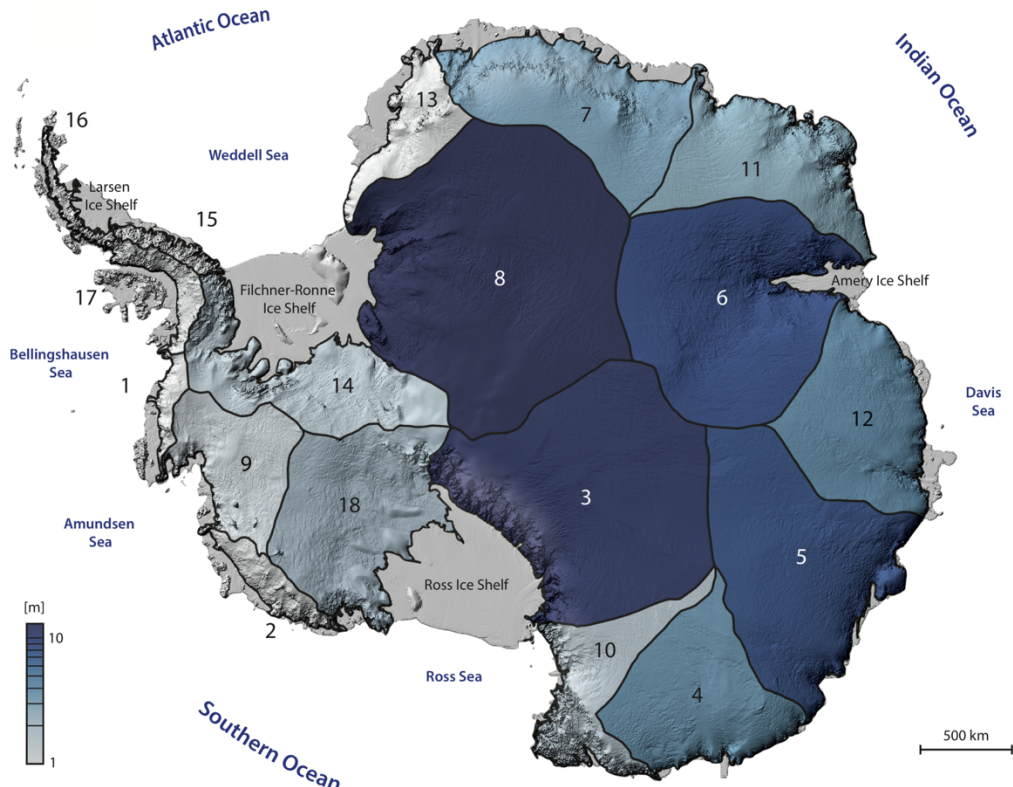
In the format provided by the authors and unedited.

Ross Ice Shelf response to climate driven by the tectonic imprint on seafloor bathymetry

K. J. Tinto^{ID 1*}, L. Padman^{ID 2}, C. S. Siddoway^{ID 3}, S. R. Springer⁴, H. A. Fricker⁵, I. Das¹, F. Caratori Tontini^{ID 6}, D. F. Porter¹, N. P. Frearson¹, S. L. Howard⁴, M. R. Siegfried^{ID 7}, C. Mosbeux⁵, M. K. Becker⁵, C. Bertinato¹, A. Boghosian¹, N. Brady⁸, B. L. Burton⁹, W. Chu^{ID 10}, S. I. Cordero¹, T. Dhakal¹, L. Dong¹, C. D. Gustafson^{ID 1}, S. Keeshin³, C. Locke^{ID 1}, A. Lockett³, G. O'Brien⁶, J. J. Spergel¹, S. E. Starke¹, M. Tankersley³, M. G. Wearing^{ID 1} and R. E. Bell¹

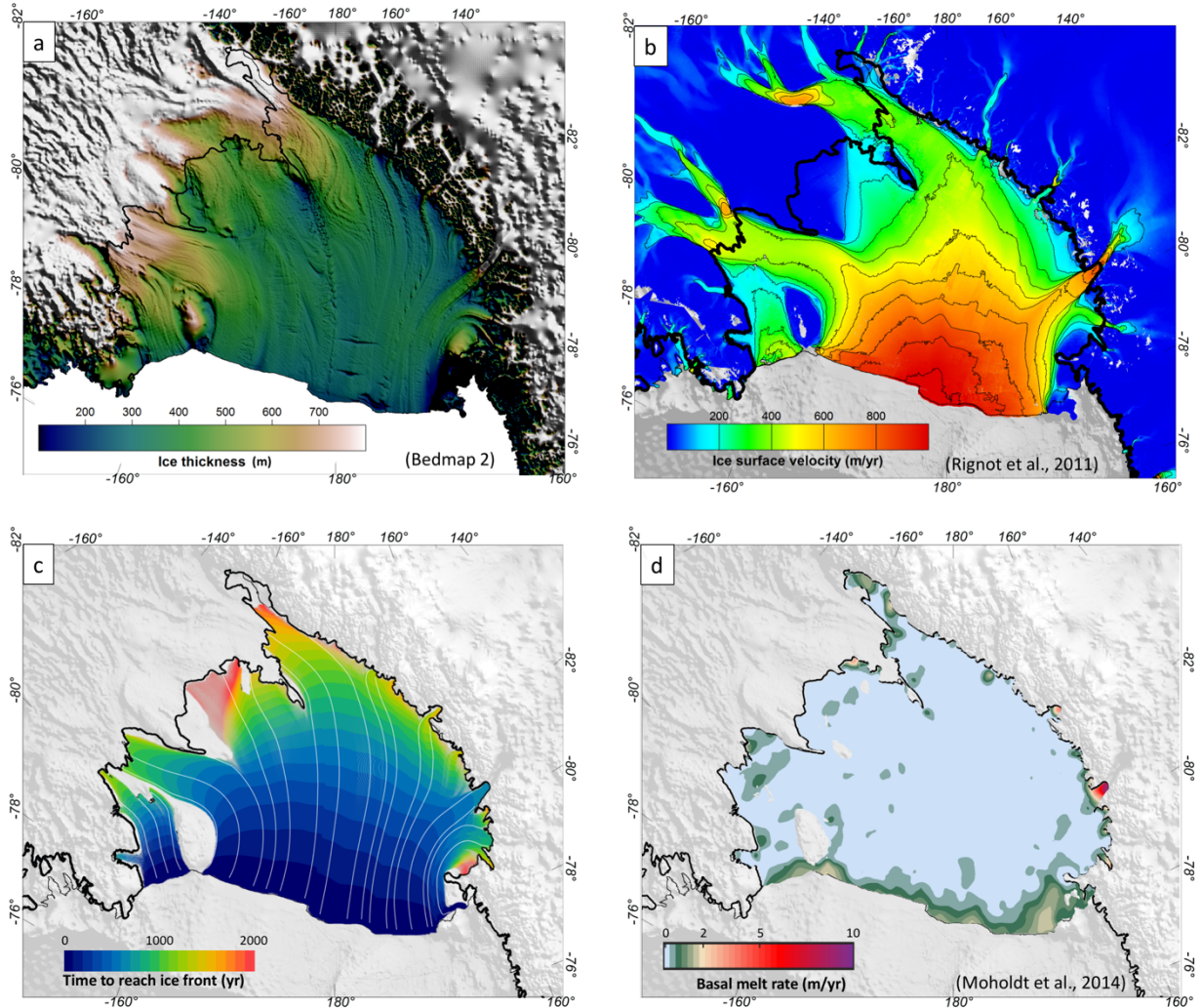
¹Lamont-Doherty Earth Observatory, Columbia University, Palisades, NY, USA. ²Earth & Space Research, Corvallis, OR, USA. ³Colorado College, Colorado Springs, CO, USA. ⁴Earth & Space Research, Seattle, WA, USA. ⁵Scripps Institution of Oceanography, University of California, San Diego, La Jolla, CA, USA. ⁶GNS Science, Lower Hutt, New Zealand. ⁷Colorado School of Mines, Golden, CO, USA. ⁸Dynamic Gravity Systems, Broomfield, CO, USA. ⁹U. S. Geological Survey, Denver, CO, USA. ¹⁰Stanford University, Stanford, CA, USA. *e-mail: tinto@ldeo.columbia.edu

Ross Ice Shelf response to climate driven by the tectonic imprint on seafloor bathymetry

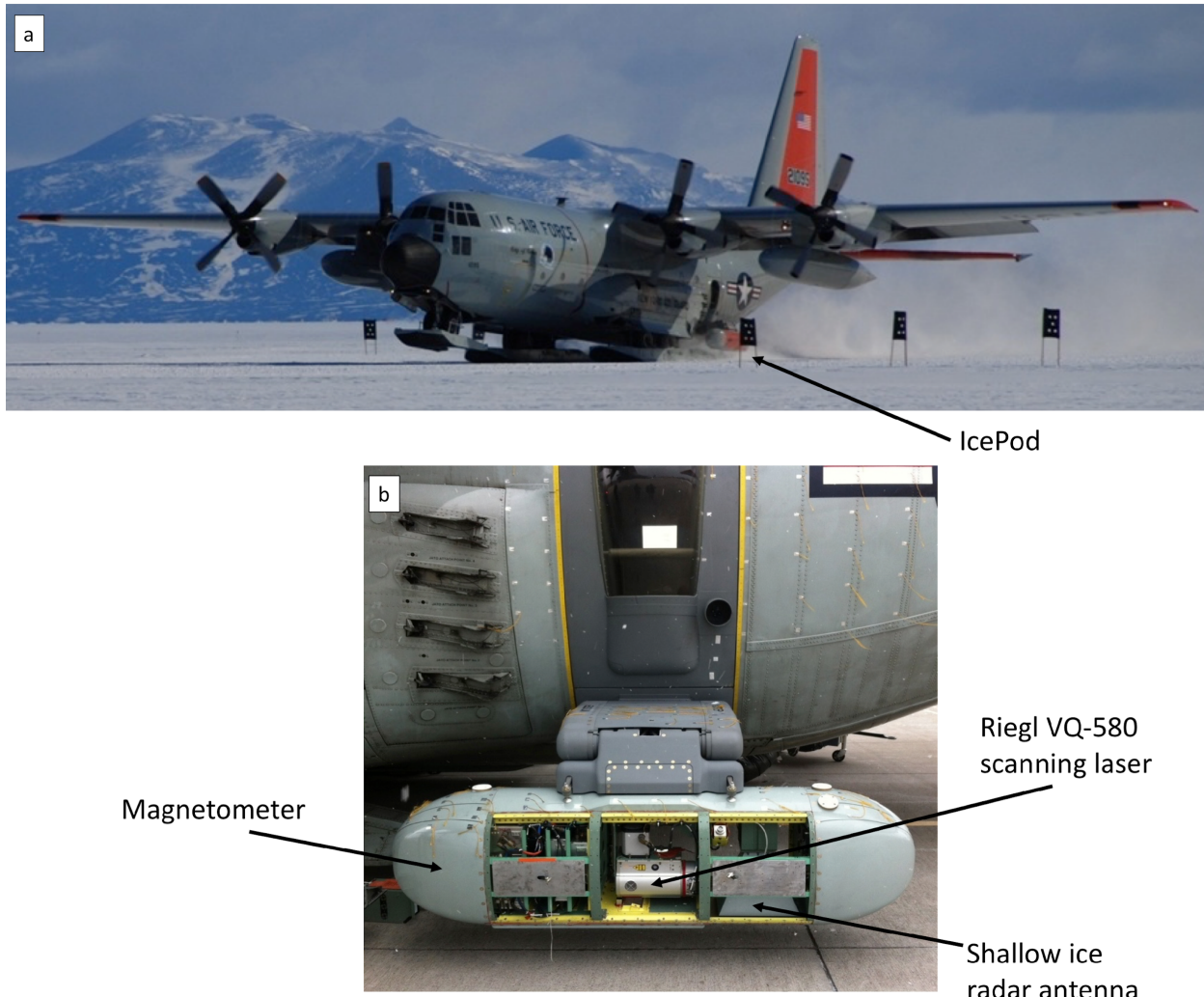


1)	0.1 m	7)	3.1 m	13)	0.7 m	Ross (basins 3 + 18): 11.6 m
2)	0.3 m	8)	12.0 m	14)	1.6 m	Filchner-Ronne (basins 8 + 14): 13.6 m
3)	9.6 m	9)	1.3 m	15)	<0.1 m	Amery (basin 6): 7.7 m
4)	3.5 m	10)	1.6 m	16)	<0.1 m	
5)	7.0 m	11)	2.7 m	17)	0.2 m	WAIS (basins 1, 2, 9, 14, 18): 5.6 m
6)	7.7 m	12)	3.7 m	18)	2.0 m	Total: 57.2 m

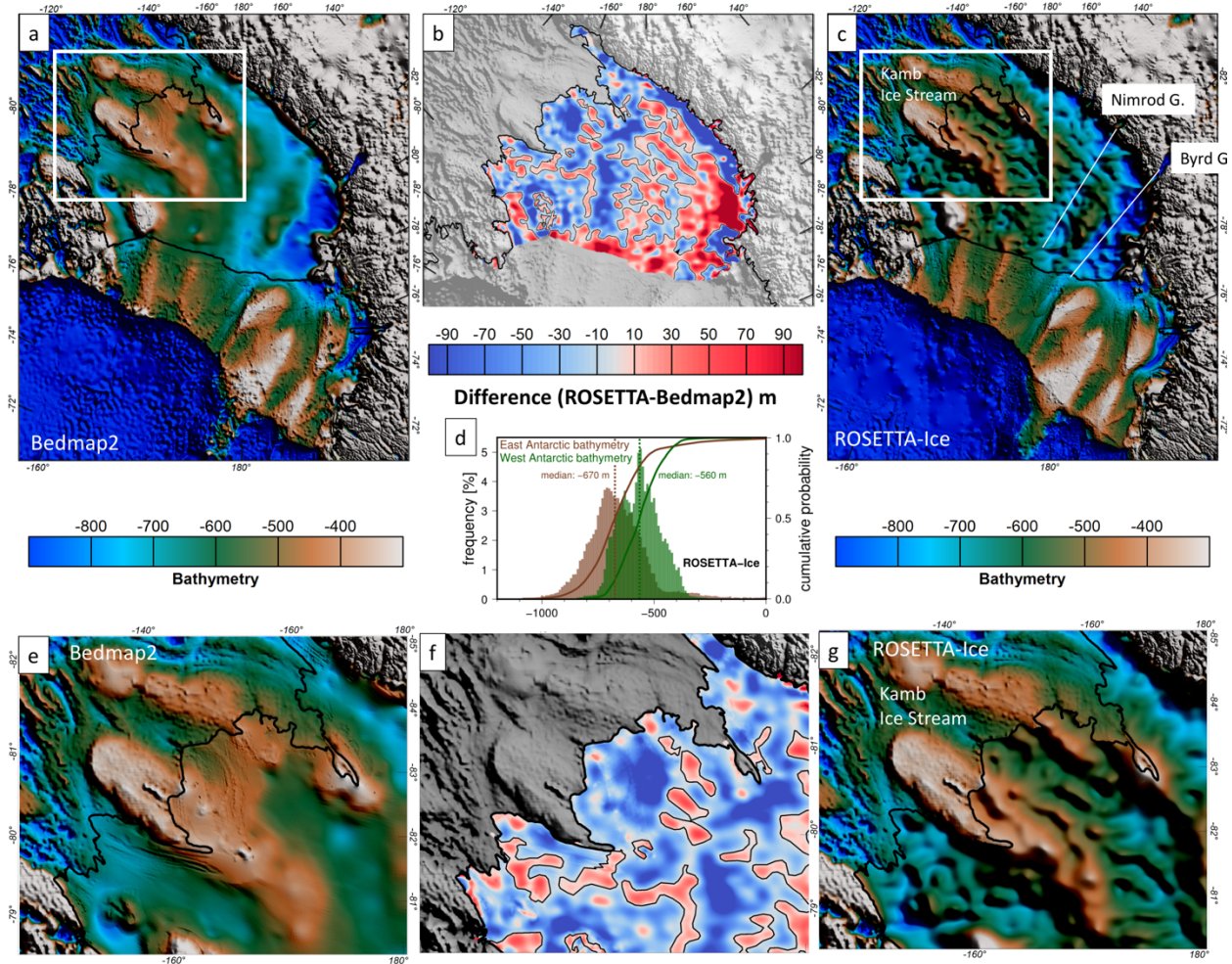
Supplementary Figure 1: Total sea level rise equivalent for each Antarctic catchment defined by Rignot et al. (2011)¹. The volume integration is computed from the ice surface and the bed topography defined in Bedmap2² then adjusted for height above floatation for marine-based regions of the ice sheet³. Summed values for catchments adjacent to large ice shelves are provided. The total for WAIS (5.6 m) exceeds the Bamber et al. (2009)³ value of 3.3 m because the latter study considered only ice that is presently grounded below sea level.



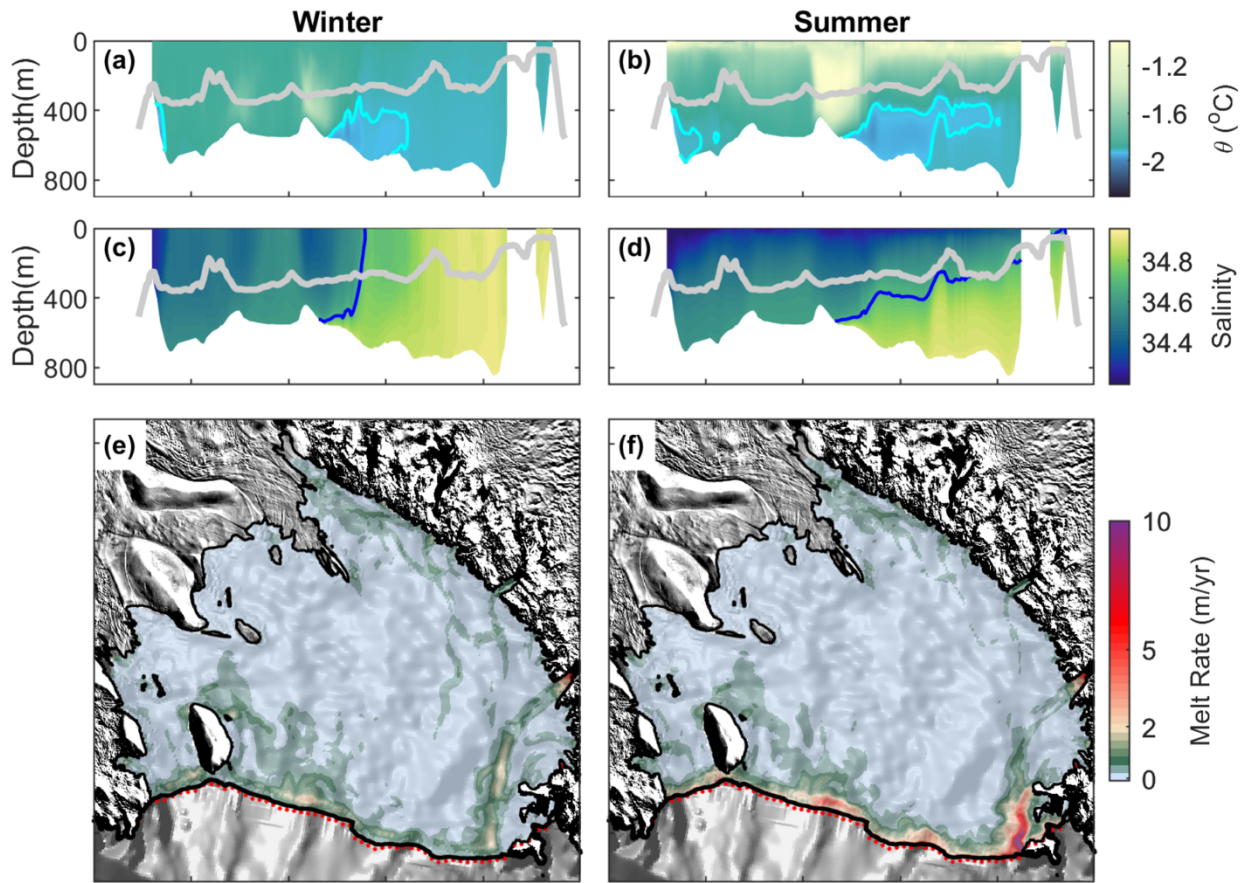
Supplementary Figure 2: Key Ice Observations across Ross Ice Shelf **a)** Ice thickness from Bedmap2. **b)** Ice surface velocity from satellite Interferometric Synthetic Aperture Radar⁴. **c)** Time for ice to travel from any point on the ice shelf to the ice shelf front, based on modern velocity field represented in **(b)**. White lines represent modern ice flowlines from the grounding line to the ice front. Ice shelf areas more than 2000 years from the ice front are unshaded. **d)** Basal melt rates derived from satellite altimetry⁵.



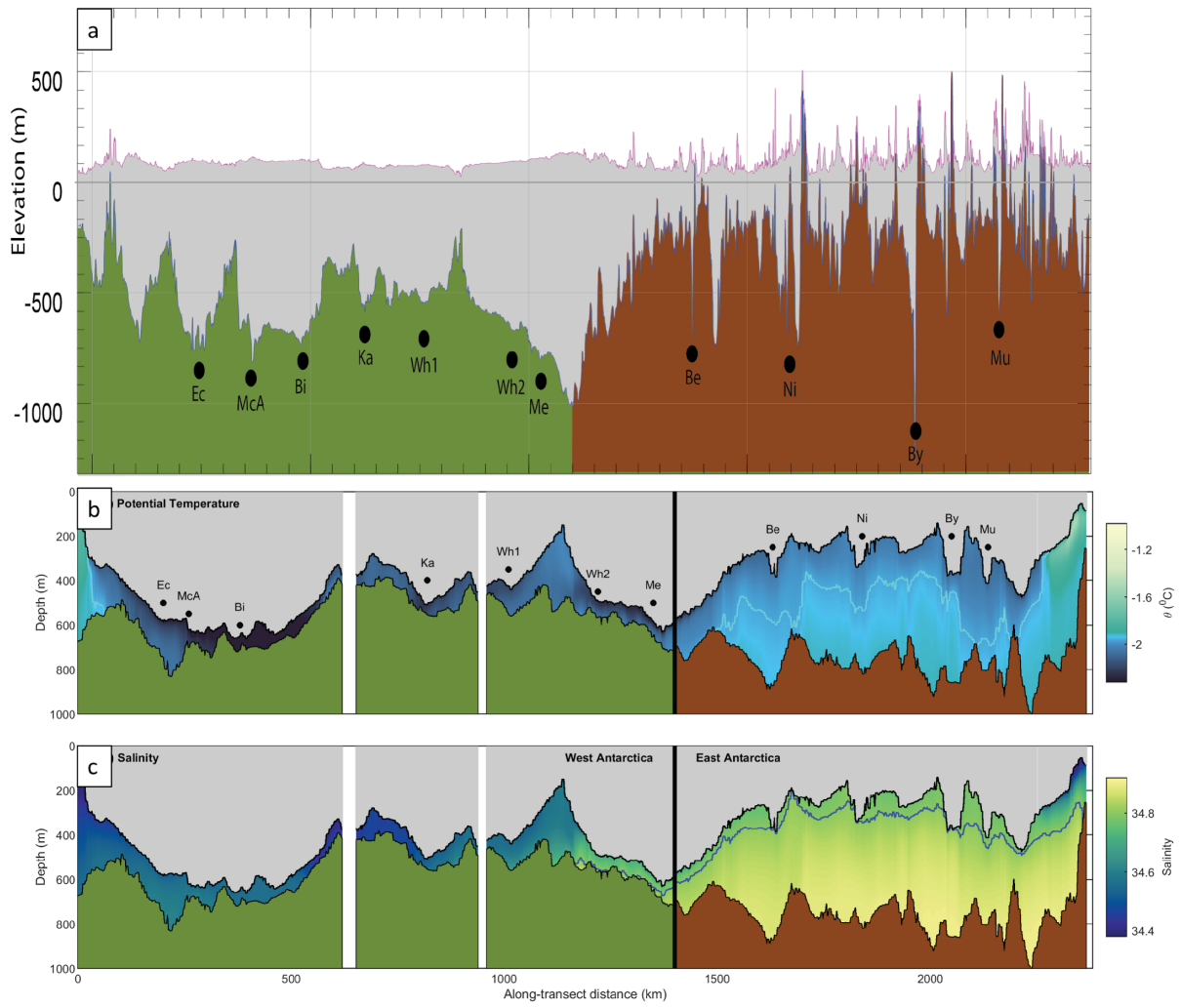
Supplementary Figure 3: The IcePod instrument suite. **a)** Location of IcePod mounted on a New York Air National Guard LC-130 (beneath the white star at rear of aircraft). **b)** Instrument arrangement (cover removed). Photo Credit: a:Mark Kurz, b:Nick Frearson).



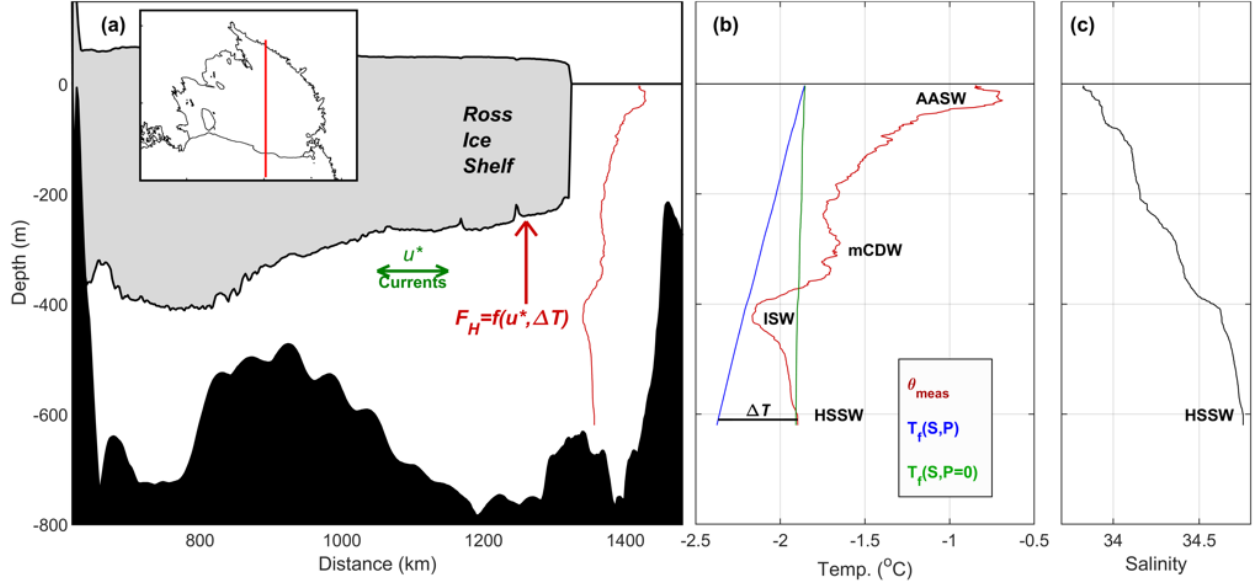
Supplementary Figure 4: Bathymetry model. Change in bathymetry between Bedmap2² compilation (a & e) and ROSETTA-Ice bathymetry model (c & g). Difference (ROSETTA-Ice minus Bedmap2) shown in b, d, and f. e – g, Expanded view of WAIS grounding line. Here the gridding algorithm used by Bedmap2 converted high-resolution features of the ice surface into the bedrock map in areas with insufficient constraints on true bathymetry. ROSETTA-Ice bathymetry removes these artifacts and reveals a much deeper bed near the grounding line of Kamb Ice Stream.



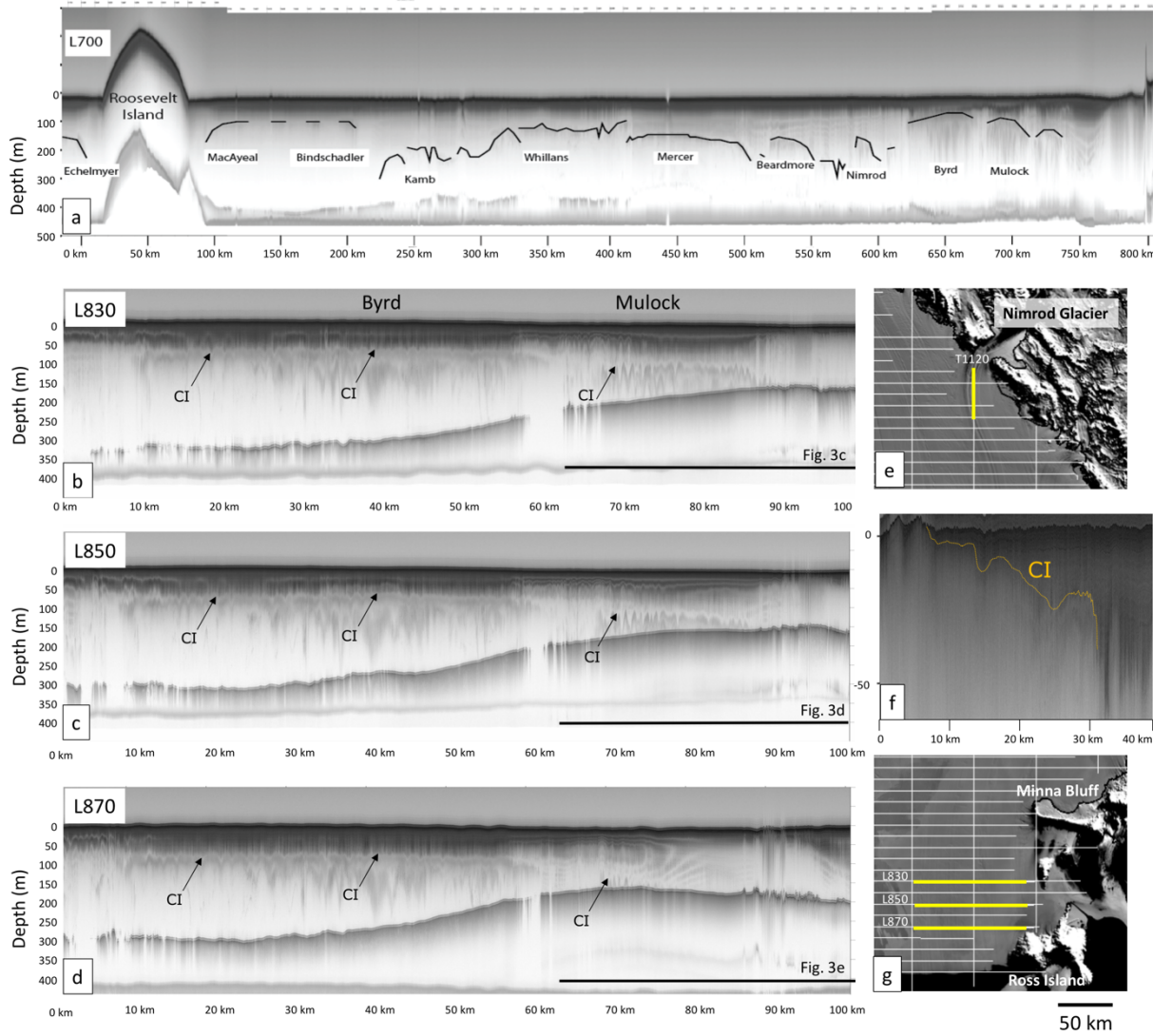
Supplementary Figure 5: Seasonal comparisons of hydrography and basal melt rates. **a & b**, Potential temperature (θ) for winter (September) and summer (February) along the ice front positions indicated by the dotted red line on (e) and (f). Cyan line outlines locations of Ice Shelf Water outflows; solid grey line is ice draft near the ice front. **c and d**, Salinity (S) for winter and summer. Blue line shows $S=34.7$, an approximate boundary for High Salinity Shelf Water. **e & f**, Basal melt rates (m/yr) from a model with atmospheric forcing and tides (Methods). High melt rates occur in summer near the ice front east of Ross Island (lower right in (f)).



Supplementary Figure 6: Grounding zone profiles **a)** Grounding line depth around Ross Ice Shelf perimeter and ice thickness from Bedmap2. Eastern limit near Cape Colbeck on left; Ross Island on right. Black dots indicate location of major ice inflows identified in Fig. 1. **b & c,** Model simulated hydrography along a transect roughly 25 km seaward of the grounding line (see Fig. 5a for location) under the Ross Ice Shelf from summer (February). **b**, Potential temperature, θ . Cyan contour is the boundary of Ice Shelf Water (ISW). **c**, Salinity. Blue contour is $S=34.7$, an approximate lower limit for High Salinity Shelf Water (HSSW). On the West Antarctic side of the Ross Ice Shelf, the cavity is thin, and contains ISW. On the East Antarctic side, the cavity is thick, and contains a layer of HSSW under ISW. Near Ross Island (right hand side), a seasonal warm, fresh layer of Antarctic Surface Water is found under shallow ice.



Supplementary Figure 7: Profiles of potential temperature (θ) and salinity (S) near the Ross Ice Shelf front. **a)** South (left) to North (right) cross-section of the ice shelf and underlying bathymetry. Inset shows location of transect. Basal melt rate is proportional to the ocean heat flux (F_H) to the ice base, where F_H is a function of friction velocity (u^*) and the temperature difference (ΔT) between the local water temperature and the in situ freezing point $T_f(S,P)$, with P being pressure. **b)** Profiles of θ , $T_f(S,P)$ and $T_f(S,P=0)$. **c**, Profile of S . Water masses are: Antarctic Surface Water (AASW, referred to in Supplementary Video M3 as Near Surface Warm Water (NSWW)); modified Circumpolar Deep Water (mCDW), the cooled extension of CDW that is present north of the continental shelf break; Ice Shelf Water (ISW); and High Salinity Shelf Water (HSSW). ISW is water with $\theta < T_f(S,P=0)$, while HSSW has $\theta \approx T_f(S,P=0)$ and $S > 34.7$. In (b), ΔT represents the thermal forcing for melting ice and, for a given value of $T(P)$, increases with depth at about $0.75^{\circ}\text{C}/\text{km}$. Near the deep grounding lines, therefore, HSSW can have potential to melt ice.



Supplementary Figure 8: Radar Profiles across Key Features

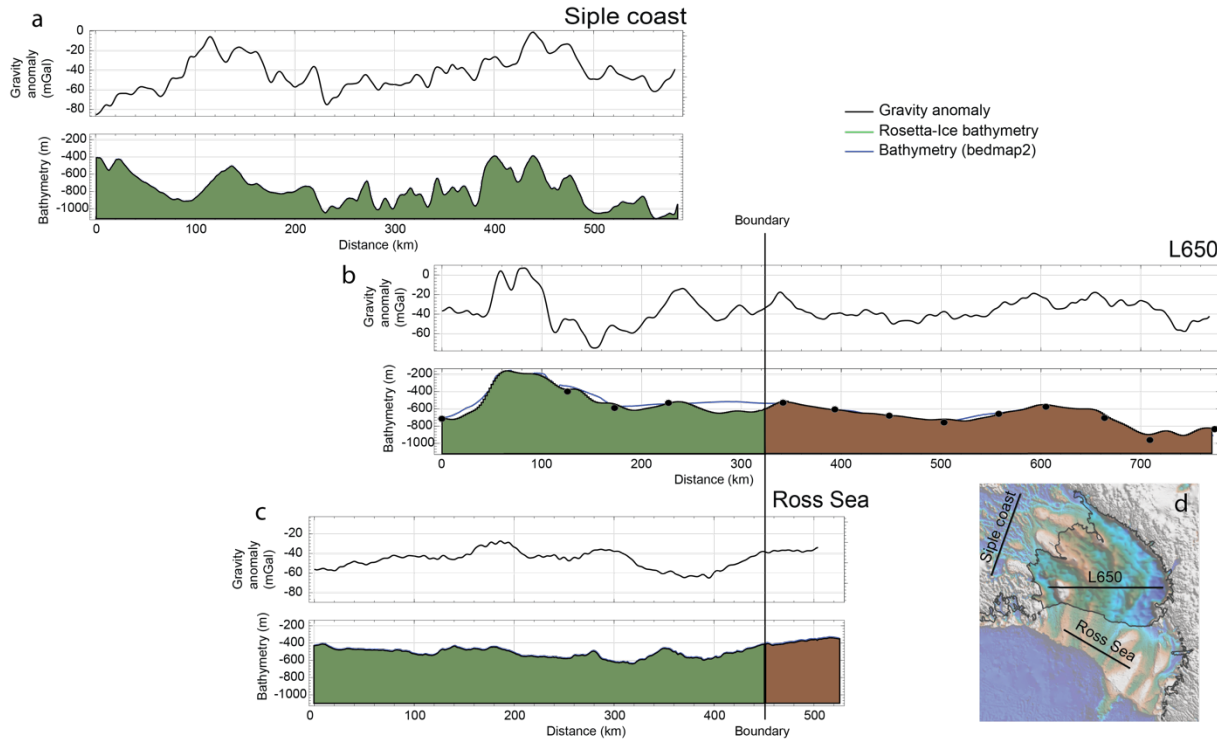
a) Shallow Ice Radar profile along ROSETTA-Ice survey line 700. Line runs from West Antarctica (on left) to East Antarctica (on right), crossing Roosevelt Island around km 10. Continental ice from flowbands corresponding to individual ice streams and glaciers can be traced along flow in the ice shelf.

b–d) Radargrams from Shallow Ice Radar, illustrating the lateral extent of thinning and removal of basal ice on the East Antarctic side of the Ross Ice Shelf. The profiles contain reflections for the continental ice of Mulock Glacier (see also Fig. 4c-e) and Byrd Glacier. For Byrd Glacier, **b–d** show a large change in continental ice thickness below the radar reflection, with the greatest change on the East Antarctic side. The change in thickness of continental ice below the radar reflections documents the thinning and removal of the basal ice layer downflow.

e) Location of flight line from **f** over MODIS image of Ross Ice Shelf.

f) Radargram of line T1120 showing Continental Ice reflector shallowing towards grounding line of Nimrod Glacier (left side of plot).

g) Location of flight lines (from **b–d**) over MODIS image of Ross Ice Shelf.



Supplementary Figure 9: Geophysical signature of Bathymetry in Ross Embayment.
 Profiles of Operation IceBridge gravity anomaly (black line) Bedmap2 bathymetry (blue) and ROSETTA_Ice bathymetry (West Antarctic crust: green, East Antarctic crust: brown) over **a**) Siple Coast **b**) Ross Ice Shelf, with RIGGS constraints (black dots) **c**) Ross Sea.

Any use of trade, firm, or product names is for descriptive purposes only and does not imply endorsement by the U.S. Government.

- 1 Rignot, E., Mouginot, J. & Scheuchl, B. Antarctic grounding line mapping from differential satellite radar interferometry. *Geophysical Research Letters* **38** (2011).
- 2 Fretwell, P. *et al.* Bedmap2: Improved ice bed, surface and thickness datasets for Antarctica. *The Cryosphere* **7**, 375-393 (2013).
- 3 Bamber, J. L., Riva, R. E., Vermeersen, B. L. & LeBrocq, A. M. Reassessment of the potential sea-level rise from a collapse of the West Antarctic Ice Sheet. *Science* **324**, 901-903 (2009).
- 4 Rignot, E., Mouginot, J. & Scheuchl, B. MEASUREs InSAR-based Antarctica ice velocity map. *Science* **333**, 1427-1430 (2011).
- 5 Moholdt, G., Padman, L. & Fricker, H. A. Basal mass budget of Ross and Filchner-Ronne ice shelves, Antarctica, derived from Lagrangian analysis of ICESat altimetry. *Journal of Geophysical Research: Earth Surface* **119**, 2361-2380 (2014).